

SYNTHESIS AND MODELLING OF FUNCTIONALIZED UiO-66 METAL-ORGANIC FRAMEWORKS FOR GAS ADSORPTION

(Sintesis dan Pemodelan Rangkaian Organik-Logam UiO-66 Terfungsi bagi Penjerapan Gas)

Tuan Nurul Azura Tuan Kob@Yaakub^{1,2}, Mohd Basyaruddin Abdul Rahman^{1,2}, Felipe Gándara⁴,
and Muhammad Alif Mohammad Latif^{1,2,3*}

¹Integrated Chemical BioPhysics Research, Faculty of Science, Universiti Putra Malaysia, 43400 UPM Serdang, Selangor, Malaysia

²Department of Chemistry, Faculty of Science, Universiti Putra Malaysia, 43400 UPM Serdang, Selangor, Malaysia

³Centre of Foundation Studies for Agricultural Science, Universiti Putra Malaysia, 43400 UPM Serdang, Selangor, Malaysia

⁴Department of New Architectures in Materials Chemistry, Materials Science Institute of Madrid – CSIC, Sor Juana Inés de la Cruz 3, Madrid, Spain

*Corresponding author: aliflatif@upm.edu.my

Received: 15 September 2023; Accepted: 25 April 2024; Published: 29 June 2024

Abstract

In this article, we present our experimental and computational findings on the adsorption of ethylene gas within variations of UiO-66 metal-organic frameworks (MOFs). UiO-66 MOF was functionalized with 2-vinylbenzoic acid (2VBA), 3-vinylbenzoic acid (3VBA), and 4-vinylbenzoic acid (4VBA) and characterized using powder X-ray diffraction techniques, FT-IR analysis and ¹H NMR. Based on structural analysis, the functionalized UiO-66 MOFs were found to possess the same structural stability as the 3D porous crystalline lattices of UiO-66, with hexanuclear zirconium oxyhydroxide clusters (Zr₆O₄(OH)₄(RCO₂)₁₂). Grand Canonical Monte Carlo simulation showed that the average loading of ethylene gas in UiO-66 and functionalized UiO-66 were relatively close. The adsorption was further investigated using radial distribution function analysis and it was found that the most favorable interactions were between the adsorbate and the carbon atom of the MOFs. These interactions were crucial for ethylene stabilization inside UiO-66 pore channels. The results presented here supported the viability of ethylene adsorption in UiO-66's modified terephthalate linker by demonstrating that functionalized UiO-66 not only retain structural integrity, but also have comparable ethylene adsorption at different pressures with stronger interactions with ethylene gas.

Keywords: metal organic framework, gas adsorption, UiO-66, Grand Canonical Monte Carlo

Abstrak

Dalam artikel ini, kami melaporkan kerja eksperimen dan hasil pengiraan untuk penjerapan gas etilena dalam rangkaian logam organik (MOF) UiO-66. UiO-66 MOF difungsikan dengan asid 2-vinilbenzoik (2VBA), asid 3-vinilbenzoik (3VBA), dan asid 4-vinilbenzoik (4VBA) serta dicirikan menggunakan teknik pembelauan sinar-X serbuk, analisis FT-IR dan ¹H NMR. Berdasarkan analisis struktur, UiO-66 MOF yang difungsikan didapati mempunyai kestabilan struktur yang sama seperti kekisi kristal berliang 3D UiO-66, dengan gugusan zirkonium oksihidroksida heksanuklear (Zr₆O₄(OH)₄(RCO₂)₁₂). Grand Canonical Monte Carlo simulasi menunjukkan purata pemuatan gas etilena dalam UiO-66 dan UiO-66 yang difungsikan adalah agak hampir hasilnya.

Penjerapan disiasat lebih lanjut menggunakan analisis fungsi taburan jejari dan didapati bahawa interaksi yang paling baik adalah antara penjerap dan atom karbon MOFs. Interaksi ini adalah penting untuk penstabilan etilena di dalam saluran liang UiO-66. Keputusan yang dibentangkan di sini menyokong daya maju penjerapan etilena dalam penyambung tereftalat yang diubah suai UiO-66 dengan menunjukkan bahawa UiO-66 yang difungsikan bukan sahaja dapat mengekalkan integriti struktur, tetapi juga mempunyai penjerapan etilena yang setanding pada tekanan yang berbeza dengan interaksi yang lebih kuat dengan gas etilena.

Kata kunci: rangkaian logam organik, penjerapan gas, UiO-66, Grand Canonical Monte Carlo

Introduction

Fast ripening and pest attack are the two most common causes of food loss in climacteric fruits. Food losses can also occur as a result of insect pest attacks in stored agricultural products. Every season, the Muda Agricultural Development Authority (MADA) estimates that RM 980 million is lost in postharvest rice crop losses [1]. As a result, solutions for controlling the ripening process and securing product storage prior to consumption are in great demand. Ethylene gas usage causes fast ripening and promotes fungal growth during storage, reducing fruit quality and shelf life [2]. As a result, for effective long-distance transportation and subsequent storage, many fruits must be kept in a low ethylene concentration environment due to its adverse effect on postharvest fruit. This has led to a great deal of research on ways to enhance ethylene adsorption and storage.

Materials used for reducing postharvest losses must be applied carefully to the targeted climacteric fruits and staple foods. Furthermore, the material's biocompatibility must be considered and created from non-toxic materials. The environmental implications, including the synthesis technique and disposal features, must also be acknowledged. For the material to be employed in food storage applications, it should ideally be water soluble or biodegradable. Ethylene gas adsorption is frequently based on extremely porous adsorbents with large surface areas, such as clays and zeolites [3]. The first porous material known to be capable of encapsulating ethylene was zeolite [4]. However, the tiny pore size of zeolite creates a significant limitation in its application on gaseous molecule exchange and release [5].

Reticular materials, or metal-organic frameworks (MOFs), are a class of functional material with unique chemical and physical characteristics. It has long been

known that MOFs, a kind of crystalline, porous material, are ideal host platforms for gas adsorption [6]. For example, copper-terephthalate (CuTPA) MOF has a total pore capacity of 0.39 cm³/g and can encapsulate 654 L/L ethylene gas in a 50 mg section of the material. When stored in a 4 L container, CuTPA loaded with ethylene dramatically accelerated the ripening of bananas and avocados [7]. One of the most used MOFs for adsorption studies is UiO-66 (Figure 1a). Numerous studies have been conducted on the adsorption of CO₂ on UiO-66, and the results have been promising [8,9]. At 298 K and 100 kPa, Le et al. (2021) discovered that UiO-66 modified with 10% PABA had the greatest CO₂ absorption capacity of 2.47 mmol g⁻¹ and ideal adsorbed solution theory (IAST)-based CO₂/N₂ selectivity, outperforming several other CO₂ benchmark adsorbents [10].

The UiO-66 metal-organic framework (MOF) has high surface area, variable pore size, and good chemical stability, making it a promising material for a wide range of applications. UiO-66 consists of 1,4-benzenedicarboxylic acid (BDC) as ligands connected by Zr₆O₈ as a metal cluster. Additionally, UiO-66 possesses easily accessible metal sites, which indicates that this material has potential applications in gas storage and separation. Due to its large specific surface area, which ranges from 1,000 to 1,500 m²/g, UiO-66 is a great choice for gas adsorption such as ethylene gas [11]. Furthermore, UiO-66 has been shown to be resistant to high temperatures (up to 500°C) and a broad range of chemical conditions, making it perfect for the adsorption of gases. By altering the metal ions or organic linkers, UiO-66's pore size may also be changed, allowing for the selective adsorption of different gas molecules [11]. Additionally, the functionalized UiO-66 can also help to increase the gasses loading and adsorption capacity. Due to UiO-66 unique properties, a great deal of research has been conducted on UiO-66

and UiO-66 mixed linker, which have been used for a range of gas adsorption and separation techniques, such as the storage of gasses, and the capture of numerous gases including ethylene, carbon dioxide, and many others. For a variety of gas-related applications, UiO-66 is a good choice due to its versatility and tunable properties.

Here, to improve adsorption capability, the UiO-66 terephthalate linker was modified with 2-vinylbenzoic acid, 3-vinylbenzoic acid and 4-vinylbenzoic acid (Figure 1c-1e). UiO-66 and functionalized UiO-66 MOFs were synthesized by using solvothermal method.

Powder X-ray diffraction techniques, FTIR analysis and ^1H NMR were used to elucidate the resulting structures. The adsorption capacity and host-guest interactions were studied using Grand Canonical Monte Carlo (GCMC) simulation. We were able to illustrate the characteristics and behaviour of ethylene adsorption within UiO-66 and functionalized UiO-66 MOFs using appropriate computational approaches to this system. Modifying the UiO-66 terephthalate linker should boost the ethylene adsorption while simultaneously increasing the number of interactions between host and guest molecules i.e., improved storage.

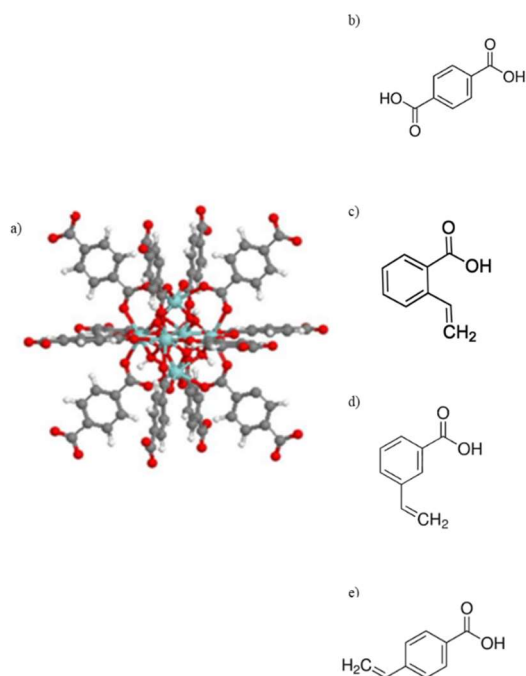


Figure 1. a) Unit cell of UiO-66, b) parent organic linker, c) 2-vinylbenzoic acid d) 3-vinylbenzoic acid, and e) 4-vinylbenzoic acid

Materials and Methods

Materials

All chemicals were obtained commercially (Aldrich) and used without further purification.

Preparation of UiO-66 and functionalized UiO-66

A standard synthesis of UiO-66 was performed by dissolving zirconium tetrachloride, ZrCl_4 (0.0625g, 6.4 mmol) in formic acid (2.5mL) and DMF (2.5mL) at room temperature in a volumetric flask. The mixture

was stirred for 20 minutes and (0.05g, 0.05mmol) 1,4-dibenzenedicarboxylic acid was added into the mixture. The mixture was stirred again for another 20 minutes. The resulting mixture was placed in an oven at $120\text{ }^\circ\text{C}$ for 24 h. After the solution cooled to room temperature in the air, the resulting solid was filtered and repeatedly washed with absolute ethanol for 3 days. Thus, the resulting white powder was filtered and dried under vacuum at ambient temperature. UiO-66 modified linker with 2-vinylbenzoic acid, 3-vinylbenzoic acid and 4-

vinylbenzoic acid were synthesized analogously by replacing 1,4-dibenzene dicarboxylic acid with ratio of 4:1 of 1,4-dibenzene dicarboxylic acid and modified linker, respectively.

Characterization

Approximately 3 mg of UiO-66 and modified samples were soaked in ethanol dispersed and dried as a thin layer on a glass plate before the PXRD measurements. PXRD data were collected at ambient atmosphere and temperature on a Bruker D5000 instrument with monochromatic Cu K α radiation ($\lambda=1.540 \text{ \AA}$) operated in Bragg-Bretano geometry. The IR experiments were performed in transmission mode on a FTIR Bruker VERTEX 80 spectrometer equipped with two detectors: a cryogenic MCT detector (spectral range 4000-600 cm^{-1}) for UiO-66 and modified UiO-66 MOFs. The MOFs under study was analyzed in the form of a thin film deposited on a silicon wafer. The thin film was prepared from an ethanol suspension of the samples. Solvent removal spectra were obtained by introducing the silicon wafer in a quartz cell that allowed *in situ* spectrum collection in a controlled atmosphere, and the sample was degassed at 373 K under dynamic vacuum (residual pressure). For the $^1\text{H-NMR}$ analysis, 20 mg of the sample were dissolved in a solution of sodium hydroxide, NaOH, and D_2O for a duration of 24 hours. The resultant solution was then utilized using a Bruker Advance DRX-300 NMR Spectrometer (300 MHz) to obtain the $^1\text{H-NMR}$ spectra.

Computational details

The UiO-66(Zr) crystal information file (.cif) with deposition number 733458 was obtained from the Cambridge Crystallographic Data Center [12]. The .cif file was utilised to carry out preliminary geometry-based analysis, such as pore sizes, using the BIOVIA Material Studio tool [13]. UiO-66 has the chemical formula $[\text{C}_{39.36}\text{H}_{23.52}\text{O}_{34.80}\text{Zr}_6]$, and the metal centers, zirconium, Zr were completely coordinated. The unit cell lengths of a, b, and c UiO-66 were 20.7343, 20.7343, and 20.7343, respectively, and the atom arrangement in the unit cell produced a triclinic symmetry. Next, using Material Studio, 2-vinylbenzoic acid, 3-vinylbenzoic acid, and 4-vinylbenzoic acid were used to modify the terephthalate acid UiO-66 linker.

Structures were modified by replacing one of the terephthalate linkers with 2-, 3-, or 4-vinylbenzoic acid using the Material Studio's "modify element" tool. The Forcite module was used to carry out energy minimization with a convergence tolerance of 10^{-4} kcal/mol. Furthermore, geometry optimization was performed using the Smart method with maximum iteration numbers of 1000 for all the MOFs series [14].

For geometry optimization, the convergence tolerances for displacement, energy, and force were set to 10^{-6} , 10^{-5} , and 10^{-4} kcal/mol, respectively. The cell parameters of the frameworks were also allowed to be relaxed at this stage. The Universal Force Field potential parameters were used to optimize UiO-66 and the functionalized UiO-66 MOFs [14]. In order to compute the electrostatic interactions between MOF atoms and the gas molecules, partial charge of the framework atoms was calculated using the Qeq (charge equilibration technique) and EQeq (extended charge equilibration method) methods, depending on the existing metal type [15]. GCMC simulations were used to examine the ethylene gas adsorption isotherms in UiO-66 and functionalized UiO-66 MOFs. All simulations were performed using the RASPA [16] package at 293 K [17] with pressures ranging from 0 to 100 kPa. The accessible pore volume and helium (He) void percentage of UiO-66, UiO-66-2VBA, UiO-66-3VBA, and UiO-66-4VBA were determined to be at 0.43, 0.44, 0.44 and 0.44 cm^3/g , respectively. Widom particle insertion was also used to calculate the He void fraction for UiO-66 and functionalized UiO-66, and the resulting values were set in the input file for adsorption simulations. A 12.0 \AA cut-off was set for electrostatic and van der Waals interactions. The adsorption simulations used up to 2.5×10^5 Monte Carlo cycles, with 5×10^4 cycles for the initial equilibrium phase and 2×10^5 cycles for the production phase [18-20]. Each Monte Carlo (MC) move was set to having an equal chance of being translated, rotated, inserted, or deleted.

Results and Discussion

Characterizations of UiO-66 and functionalized UiO-66

The powder X-ray diffraction (PXRD) pattern of the synthesized UiO-66 and functionalized UiO-66 MOFs

are shown in Figure 2. The peaks are identical to the one previously reported research [21]. The identical XRD patterns of UiO-66 and functionalized UiO-66 show that these functionalized UiO-66 have the same 3D porous crystalline lattices as UiO-66, with hexanuclear zirconium oxyhydroxide clusters ($Zr_6O_4(OH)_4(RCO_2)_{12}$) and octahedral cages assembled with these modified terephthalate linkers. It was determined that the functionalization did not alter the framework topology of UiO-66(Zr) MOFs. The peak at $2\theta = 7.3^\circ$ corresponds to the (111) crystal plane of the UiO-66 structure. This peak is one of the important peaks for UiO-66 and this peak was considered as

fingerprint peak that indicates whether a sample has the UiO-66 framework. When compared to another UiO-66 sample, the peak for UiO-66-2VBA at 7.3° is sharper and more intense, indicating that the UiO-66-2VBA sample has good crystallinity properties. A second notable low-angle peak is seen at approximately $2\theta = 8.4^\circ$, which is the crystal plane (200). Additionally, mid-angle peaks were noted at around $2\theta = 12.0^\circ$, which is the peak associated with the (220). The (311) crystal plane is assigned a peak at about $2\theta = 14.0^\circ$. The (222) crystal plane is thought to be responsible for the peak at about $2\theta = 15.8^\circ$.

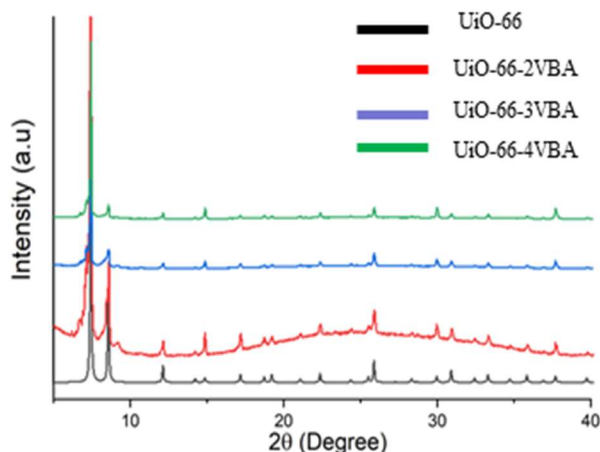


Figure 2. PXRD pattern for UiO-66 and functionalized UiO-66

The FT-IR spectra of UiO-66 and functionalized UiO-66 MOFs is shown in Figure 3. These four UiO-66 samples have IR spectra with comparable distinctive peaks. UiO-66 sample FTIR spectra show multiple major wavelengths. We can see a large peak around 3419 cm^{-1} that indicated -OH group present in the structure. Two highly linked C-O bonds in the carboxylate group of the ligand, BDC, result in two distinct peaks: an asymmetric C-O stretching band at 1586 cm^{-1} and a symmetric C-O stretching band at 1398 cm^{-1} . The C=C of the benzene ring of the ligand in the structure could be the source of the tiny bands at 1504 cm^{-1} . After synthesizing UiO-66 using a mixed linker, the peaks show that the ligand at 1586 cm^{-1} changed somewhat and widened. The existence of several functional groups with various vibrational frequencies, which cause overlapping bands and a broadening effect,

is one potential explanation.

Solid state ^1H NMR of the three UiO-66-2VBA, UiO-66-3VBA and UiO-66-4VBA samples also exhibit similar characteristic peaks with the one previously reported [22]. According to Ky Vo et al. (2020) ^1H NMR spectra, UiO-66 had a single signal that was 7.84 ppm in strength and was attributed to the phenyl proton of the BDC ligand [23]. On the other hand, our research indicates that functionalized UiO-66 show three distinct peaks (Figure 4). The ^1H NMR spectra of functionalized UiO-66 show two notable peaks: one at 1.9 ppm, which is related to the vinyl chain, and another at 7.8 ppm, which is related to the aromatic protons in the ligand. The addition of vinyl groups to the UiO-66 framework is linked to the different peaks observed in the ^1H NMR spectra of the functionalized UiO-66. A noteworthy

peak was noted for the functionalized UiO-66. The result of bridging hydroxyl (OH) protons is a wide

singlet at 5.5 ppm, which represents the four hydroxyl protons that bridge the zirconium clusters.

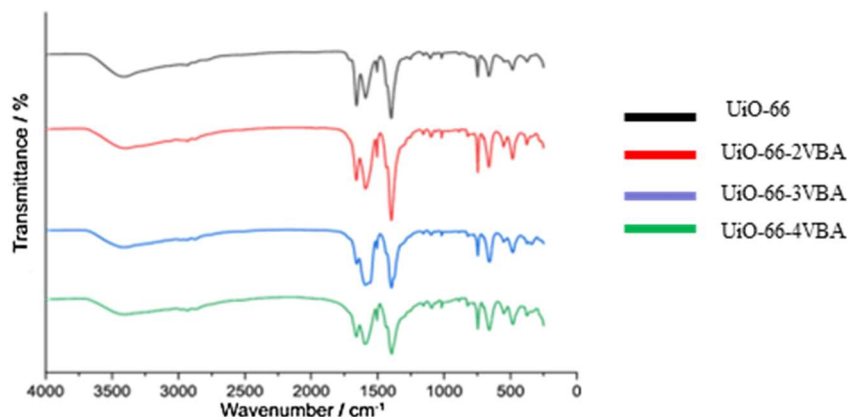


Figure 3. FT-IR spectra for UiO-66 and UiO-66 with mixed linker

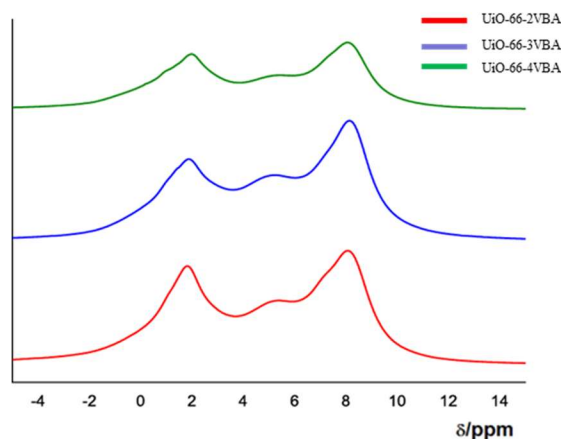


Figure 4. ¹H NMR Spectra of UiO-66 functionalized

Adsorption isotherm

Figures 5(a) and 5(b) show the ethylene gas adsorption isotherms in UiO-66 and functionalized UiO-66 at 293 K. Force fields mentioned in the method section were used and the ethylene uptake was simulated at pressures ranging from 0 to 100 kPa. The average loading for UiO-66 and functionalized UiO-66 rose as the pressure increased from 0 kPa to 100 kPa. When the MOFs are sorted according to the average loading for molecule per unit cell, the following order were produced; UiO-66-2VBA > UiO-66-4VBA > UiO-66-3VBA > UiO-66. At 100kPa, the maximum ethylene gas loading was 14.45 molecules per unit cell in UiO-66-2VBA, as compared

to 14.05, 14.37, and 14.40 molecules per unit cell in UiO-66, UiO-66-3VBA, and UiO-66-4VBA, respectively. Although the highest loading was found for UiO-66-2VBA, the values between all MOFs were closely spaced. The present of the guest-guest interactions, which played a key role at higher pressures resulting in larger loadings, may explain the small variation in the average ethylene loading. The observations at higher pressures do not truly reflect the functionalized UiO-66's remarkable sensitivity to isotherms. Hence, the intermolecular interactions analysis was carried out to better understand the influence of functionalization on ethylene gas

adsorption.

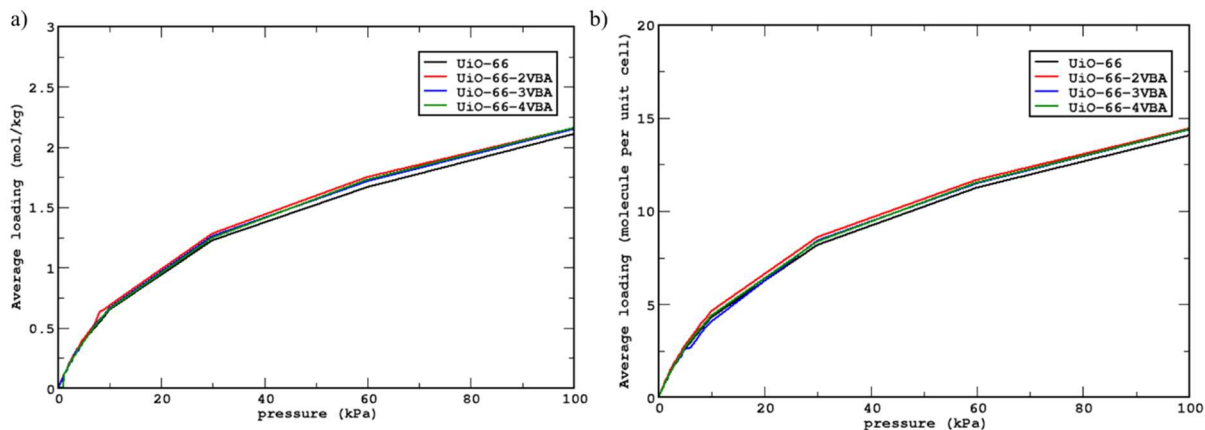


Figure 5. Simulated adsorption isotherms of ethylene molecule in UiO-66 and functionalized UiO-66: (a) pressure(kPa) versus average loading (mol/kg) and (b) pressure(kPa) versus average loading (molecule per unit cell)

Radial Distribution Function (RDF)

To study the interactions of the ethylene gas with UiO-66 and functionalized UiO-66 MOFs, the radial distribution function (RDF) was calculated using the following equation:

$$g_{ij}(r) = \frac{N_{ij}(r, r + \Delta r) \cdot V}{4\pi r^2 \cdot \Delta r \cdot N_i \cdot N_j} \quad (1)$$

In this equation, $N_{ij}(r, r + \Delta r)$ represents the number of particles j around particle i inside the area from r to $r + \Delta r$. V and N denote the volume of the system and the number of particles, respectively. Analyzing RDF allowed for assessing the distribution of ethylene gas molecules on the interaction sites of UiO-66 and functionalized UiO-66 MOFs. In general, the greatest distribution of gas molecules in the UiO-66 pores must follow the adsorbed quantity. The RDF plots for ethylene gas (Figure 6) showed an acceptable distribution of oxygen, hydrogen, carbon and zirconium atoms based on the adsorbed quantities and van der Waals surfaces of UiO-66 and functionalized UiO-66 MOFs. Although the ethylene gas adsorption quantity in UiO-66 and functionalized UiO-66 MOFs is not significantly different, the difference in terms of RDF values is noticeable. The level of distribution for the gas molecules was found in the order of $\text{UiO-66-2VBA} < \text{UiO-66-4VBA} < \text{UiO-66} < \text{UiO-66-3VBA}$ (Figure 6). Except for UiO-66, these results show an agreement

with the adsorption isotherm results. Carbon, C and Zr atoms in the UiO-66-2VBA were discovered to be the most favorable sites for ethylene gas. C and Zr atoms have distribution $g(r)$ values of 3.1 and 3.5 in UiO-66-2VBA, respectively. In comparison, the $g(r)$ distributions for C and Zr atoms in UiO-66 are only approximately 2.0 and 3.1, respectively. These findings show that functionalizing UiO-66 with vinyl benzoic acid increased the interaction of ethylene gas with the C of the organic linker, while decreasing the interaction with H atoms.

Simulation snapshot analysis

The simulation snapshots for the adsorption of the ethylene gas in UiO-66, UiO-66-2VBA, UiO-66-3VBA and UiO-66-4VBA at 100 kPa along the y-axis is presented in Figure 7. As illustrated, all gas molecules were contained within pores of UiO-66. The simulated snapshots show molecules of ethylene gas adsorbed in UiO-66's porous structure. The ethylene molecules are located at the centre of the huge channels, where they interact with the framework via van der Waals forces. UiO-66's huge pore size enable effective ethylene adsorption, which results in a high adsorption capacity. The snapshots also indicate that ethylene gas molecules were adsorbed on the exposed zirconium metal sites. This Lewis's acid sites, which are made from coordinatively unsaturated zirconium atoms, facilitate robust interactions with the ethylene molecules. The

figure further shows that ethylene gas molecules are also dispersed throughout the framework, taking up the available pore space of UiO-66. It also can be observed that the functionalization of UiO-66 with vinyl benzoic acid helps to enhance the active sites for ethylene gas interactions. More ethylene gasses were adsorbed in the framework's pore in UiO-66-2VBA, UiO-66-3VBA, and UiO-66-4VBA. This might be owing to increased interactions between ethylene and the linker in the framework. It was clear that functionalizing UiO-66 had

a positive effect on the adsorption of ethylene. As the pressure increased, the framework was gradually loaded with ethylene molecules at the metal sites. Hence, interactions between ethylene gas and Zr metal ions also increase. In comparison, the ethylene molecules' interaction with the UiO-66-2VBA framework is stronger than that of UiO-66, UiO-66-3VBA, and UiO-66-4VBA adsorption. This suggests that the ethylene gas adsorption inside UiO-66 MOF is enhanced by the mixed linker techniques.

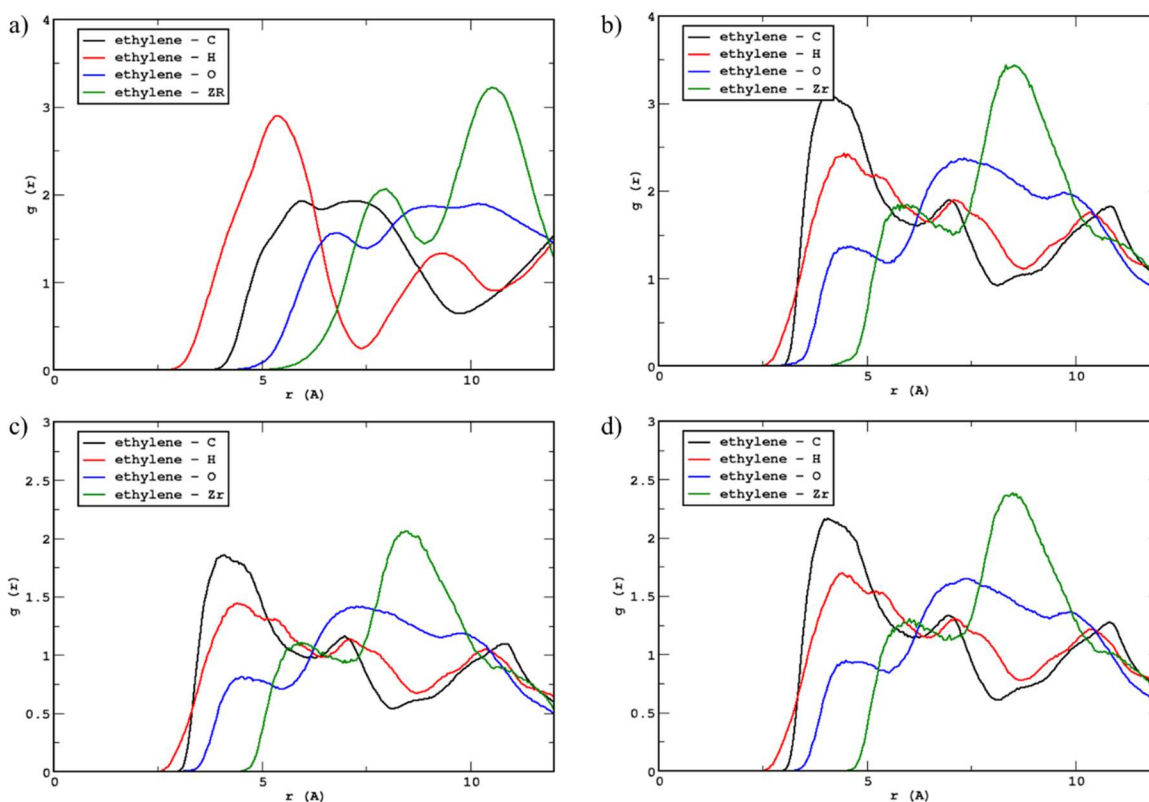


Figure 6. Radial distribution plots for (a) UiO-66, (b) UiO-66-2VBA, (c) UiO-66-3VBA, and (d) UiO-66-4VBA

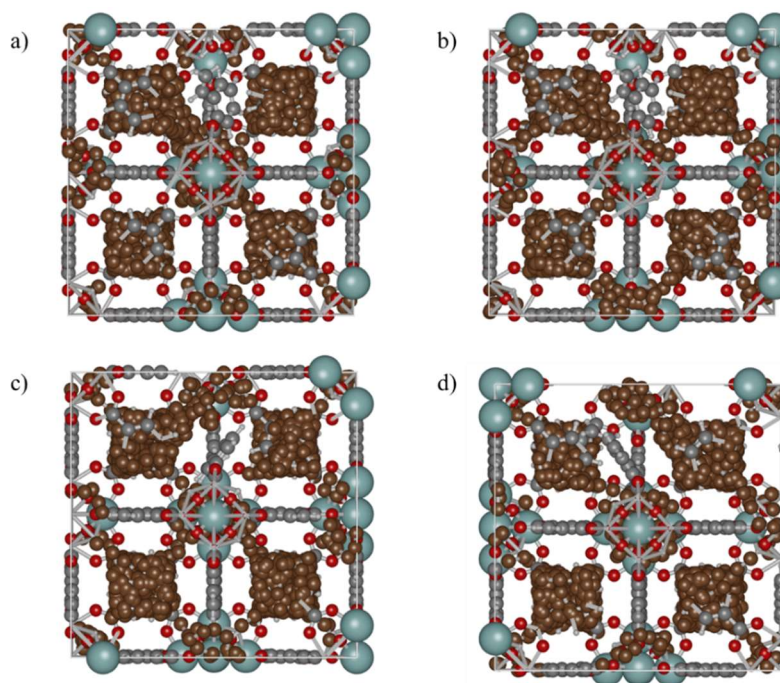


Figure 7. Simulation snapshot for (a) UiO-66, (b) UiO-66-2VBA, (c) UiO-66-3VBA, and (d) UiO-66-4VBA at 100kPa. The colors in the snapshot correspond to: linkers (grey), Zirconium atom (light blue), Oxygen atom (red) and ethylene gasses (brown)

Conclusion

We have successfully synthesized three functionalized, UiO-66 MOFs. The functionalization with different variations of vinyl benzoic acid did not disrupt the overall framework topology of the UiO-66(Zr) MOF. GCMC simulations provided an atomic-level understanding of ethylene gas adsorption in UiO-66, UiO-66-2VBA, UiO-66-3VBA, and UiO-66-4VBA at pressures ranging from 0 kPa to 100 kPa. The adsorption isotherm revealed the largest and most consistent ethylene loading in UiO-66-2VBA but did not differ significantly from the other MOFs studied. The carbon atoms in the functionalized linker and the Zr metal ion have the most interactions with ethylene gases. This was validated further by analyzing the simulation snapshots at 100kPa. Based on the findings, we determined that functionalization of UiO-66 MOF with vinyl benzoic acid will contribute towards more efficient ethylene gas adsorption and storage.

Acknowledgement

The authors would like to acknowledge the Ministry of Education (MOE) Malaysia. This research is supported

by the Ministry of Education (MOE) Malaysia through Fundamental Research Grant Scheme (FRGS/1/2020/STG04/UPM/02/9). We are grateful to Dr. Felipe Gándara Barragan (ICMM, Madrid) for his support of global science activities.

References

1. Che Omar, S., Shaharudin, A., and Tumin, S.A. (2019). The status of the paddy and rice industry in Malaysia. *In Khazanah Research Institute*.
2. Saltveit, M.E. (1999). Effect of ethylene on quality of fresh fruits and vegetables. *Postharvest Biology and Technology*, 15: 279-292.
3. Sehaqui, H., Zhou, Q., and Berglund, L.A. (2011). High-porosity aerogels of high specific surface area prepared from nanofibrillated cellulose (NFC). *Composites Science and Technology*, 71: 1593-1599.
4. Golipour, H., Mokhtarani, B., Mafi, M., Moradi, A.V., and Godini, H.R. (2020). Experimental measurement for adsorption of ethylene and ethane gases on copper-exchanged zeolites 13X and 5A. *Journal of Chemical & Engineering Data*, 65:

- 3920-3932.
5. Cao, Z., Anjekar, N.D., and Yang, S. (2022). Small-pore zeolite membranes: A review of gas separation applications and membrane preparation. *Separations*, 9: 47.
 6. Li, B., Wen, H.M., Zhou, W., and Chen, B. (2014). Porous metal-organic frameworks for gas storage and separation: what, how, and why? *The journal of physical chemistry letters*, 20: 3468-3479.
 7. Zhang, B., Luo, Y., Kanyuck, K.M., Bauchan, G.R., Mowery, J.D., and Zavalij, P.Y. (2016). Development of metal-organic framework for gaseous plant hormone encapsulation to manage ripening of climacteric produce. *Journal of Agricultural and Food Chemistry*, 23: 5164-5170.
 8. Grissom, T.G., Driscoll, D.M., Troya, D., Sapienza, N.S., Usov, P.M., Morris, A.J., and Morris, J.R. (2019). Molecular-level insight into CO₂ adsorption on the zirconium-based metal-organic framework, UiO-66: A combined spectroscopic and computational approach. *The Journal of Physical Chemistry C*, 22: 13731-13738.
 9. Ethiraj, J., Albanese, E., Civalleri, B., Vitillo, J.G., Bonino, F., Chavan, S.M., Shearer, G.C., Lillerud, K.P., and Bordiga, S. (2014). Carbon dioxide adsorption in amine-functionalized mixed-ligand metal-organic frameworks of UiO-66 topology. *ChemSusChem*, 12: 3382-3388.
 10. Le, V.N., Vo, T.K., Yoo, K.S., and Kim, J. (2021). Enhanced CO₂ adsorption performance on amino-defective UiO-66 with 4-amino benzoic acid as the defective linker *Separation and Purification Technology*, 274: 119079.
 11. Zhao, W., Zhang, C., Yan, Z., Zhou, Y., Li, J., Xie, Y., Bai, L., Jiang, L., and Li F. (2017). Preparation, characterization, and performance evaluation of UiO-66 analogues as stationary phase in HPLC for the separation of substituted benzenes and polycyclic aromatic hydrocarbons. *PLoS One*.
 12. Trouselet, F., Archereau, A.Y., Boutin, A., and Coudert, F. (2016). Heterometallic metal-organic frameworks of MOF-5 and UiO-66 families: Insight from computational chemistry. *Journal of Physical Chemistry C*, 120: 24885-24894.
 13. Dassault Systèmes BIOVIA, B. W. *Release 2017; BIOVIA Pipeline Pilot, Release 2017*; Dassault Systèmes, San Diego, CA.
 14. Rappe, A. K., Casewit, C. J., Colwell, K. S., Goddard, W. A., and Skiff, W. M. (1992). UFF, a full periodic table force field for molecular mechanics and molecular dynamics simulations. *Journal American Chemical Society*, 114: 10024,
 15. Wilmer, C. E., Kim, K. C., and Snurr, R. Q. (2012). an extended charge equilibration method. *Journal of Physical Chemistry*, 3: 2506-2511.
 16. Dubbeldam, D., Calero, S., Ellis, D.E., and Snurr, R.Q. (2016). RASPA: Molecular simulation software for adsorption and diffusion in flexible nanoporous materials. *Journal of Molecular Simulation*, 42: 81-101.
 17. Savage, M., Yang, S., Suyetin, M., Bichoutskaia, E., Lewis, W., Blake, A.J., Barnett, S.A., and Schröder, M. A. (2014). Novel bismuth-based metal-organic framework for high volumetric methane and carbon dioxide adsorption. *Journal of Chemical European*, 20: 8024-8029.
 18. Xia, X., Hu, G., Li, W., and Li, S. (2019). Understanding reduced CO₂ uptake of ionic liquid/metal organic framework (IL/MOF) composites. *Journal of Applied Nano Material*, 2: 6022-6029.
 19. Anderson, R., Schweitzer, B., Wu, T., Carreon, M.A., and Gómez-Gualdrón, D.A. (2018). Molecular simulation insights on Xe/Kr separation in a set of nanoporous crystalline membranes. *Journal of Applied Material Interfaces*, 10: 582-592.
 20. Avci, G., Velioglu, S., and Keskin, S. (2018). High-throughput screening of MOF adsorbents and membranes for H₂ purification and CO₂ capture. *Journal of Applied Material Interfaces*, 10: 33693-33706.
 21. Rahmawati, I., Ediaty, R., and Prasetyoko, D. (2014). Synthesis of UiO-66 using solvothermal method at high temperature. *Journal of Proceedings Series*, 1: 2354-6026.
 22. Vakili, R., Xu, S., Al-Janabi, N., Gorgojo, P., Holmes, S.M., and Fan, X. (2018). Microwave-assisted synthesis of zirconium-based metal organic frameworks (MOFs): Optimization and gas

- adsorption. *Microporous and Mesoporous Materials*. 260: 45-53.
23. The Ky, V., Le, V. N. N., Van, S., Mugeun, K., Daekeun, Y., Kye, S., Park, B., and Kim, J. (2020). Microwave-assisted continuous-flow synthesis of mixed-ligand UiO-66(Zr) frameworks and their application to toluene adsorption. *Journal of Industrial and Engineering Chemistry*. 86: 178-185.